Proceedings of the 12th International Conference "Ion Implantation and Other Applications of Ions and Electrons", ION 2018

Microstructural Effects of Al Doping on Si_3N_4 Irradiated with Swift Heavy Ions

A. Janse van Vuuren[a,*], V. Skuratov[b], A. Ibrayeva[c] and M. Zdorovets[c]

[a]Centre for HRTEM, Nelson Mandela University, University Way, Summerstrand, Port Elizabeth, 6031, South Africa

[b]Flerov Laboratory for Nuclear Research, Joint Institute for Nuclear Research, Joliot-Curie 6, Dubna, 141980, Moscow region, Russia

[c]The Institute of Nuclear Physics, 1 Ibragimova Str., Almaty, 050032, Republic of Kazakhstan

Transmission electron microscopy techniques were used to investigate the effect of swift xenon ions on the microstructure of polycrystalline Al doped β -Si_3N_4. The target material was irradiated with Xe with energies between 167 and 220 MeV with initial stopping powers of 20 and 22 keV/nm, respectively. The fluences ranged between 3×10^{11} to 6×10^{14} cm^{-2} and irradiation was done at room temperature. The formation of discontinuous latent ion tracks was observed in all samples. The threshold stopping power for track formation in Al doped β -Si_3N_4 was determined to be approximately 8.9 keV/nm and the threshold fluence for amorphisation due to electronic stopping in the range between 1×10^{13} and 2×10^{14} cm^{-2} at a threshold stopping power of between 6.8 and 8.1 keV/nm. It was also found that the doping of β -Si_3N_4 with Al lowers the threshold for amorphisation as compared to pure β -Si_3N_4.

DOI: 10.12693/APhysPolA.136.241

PACS/topics: 01.30.Cc, 07.78.+s, 61.80.Jh, 61.82.Fk

1. Introduction

The storage of nuclear waste products is a major concern of the nuclear industry. The ideal case would be to develop technologies which can eventually enable a partially- or fully-closed nuclear fuel cycle. This may include the reprocessing or alternative re-integration of nuclear waste products into the fuel cycle.

Inert matrix fuel for the burn-up of plutonium and other minor actinides (MAs) is one of these proposed technologies currently under development. Inert matrix fuel involves the embedding of Pu and/or MAs in an inert matrix material in either a solid solution formation or a two-phase microstructure [1]. To determine the viability of candidate materials to use as inert matrices, their radiation tolerance to various sources of radiation need to be quantified. The types of radiation within the reactor core include fission fragments (FFs), α -particles, γ -rays, etc. [1, 2].

The effects of FFs on the material microstructure is one of the qualifying criteria for inert matrices. Swift heavy ions (SHIs) are ideal for the simulation of FF radiation, because they have masses and energies comparable to those of FFs. The microstructural changes in the irradiated material are studied within the current theoretical framework describing the interaction of SHIs with solids, called the thermal spike model [3]. Heavy ions with energies > 100 keV/nucleon lose energy primarily by inelastic energy transfer mechanisms to the electronic subsystem of the target material which may lead to the formation of latent ion tracks in some materials. Latent tracks may be amorphous, and may contain defects of a different phase than the unaffected material. The effects of ion irradiation on the microstructure of materials is of interest to both science and technology. In nuclear applications radiation effects limit the lifetime of reactor materials. The modelling and prediction of microstructural modification resulting from ion irradiation therefore holds considerable benefit [4].

The current investigation revolves around β -Si_3N_4, a ceramic which has an excellent combination of thermal (the thermal conductivity can range between 40–155 W/(m K), depending on the purity, grain size, and grain boundary film thickness [5]), electrical, and mechanical properties including a high melting temperature ($\approx$ 1900 °C), good oxidation and corrosion resistance, and also high strength at both room and elevated temperatures. Si_3N_4 can exist in three crystal structures α -(trigonal), β -(hexagonal), and γ -phase (cubic). α-and β -phase are the most common forms of Si_3N_4 [6, 7].

2. Materials and methods

Commercially available polycrystalline β-Si_3N_4 obtained from MTI corporation was used in this investigation. High energy ion irradiation of these samples was performed with the IC-100 cyclotron at the FLNR at the JINR in Dubna, Russia and with the DC-60 cyclotron at the IRC in Astana, Kazakhstan. The target materials were irradiated with Xe ions with energies ranging from 167 to 220 MeV and fluences between

*corresponding author; e-mail: arnojvv@gmail.com

3×10^{11} and 6×10^{14} cm^{-2}. Cross-sectional TEM lamella were prepared by means of an FEI Helios Nanolab 650. To minimise ion beam induced damage the samples were prepared with ion energies down to 500 V. Structural and compositional analysis was done with either a JEOL JEM 2100 LaB_6 or ARM200F transmission electron microscope (TEM) operated at 200 kV. The TEM analysis included selected area diffraction (SAD) and energy dispersive X-ray spectrometry (EDS).

3. Results

The Si_3N_4 used in this investigation is a polycrystalline sintered material. The sintering compound consists mainly of Al and O with a small amount of Y also present. EDS analysis of the material shows that most of the Si_3N_4 grains contain a small amount of Al most likely due to the sintering process. EDS analysis showed only a small amount of Al, compared to Si. Modeling of the doping of Si_3N_4 indicates that Al can substitute Si and also occupy certain interstitial sites within the lattice [8–10]. The doping of a materials with even small amounts of some elements can cause very specific alterations to the mechanical, thermal, and electronic properties of a material [9–11].

In this investigation the main goal is to study the microstructural response of Si_3N_4 to high energy heavy ions where the transfer of energy is through electronic stopping mechanisms and specifically the effect of Al doping on Si_3N_4 in this regard.

In Fig. 1a latent tracks can be seen to have formed as a consequence of irradiation with 167 MeV Xe ($S_e \approx 20$ keV/nm), they are visible as bright-dotted lines where the crystals appear darker and as dark-dotted lines where the crystals appear lighter. At this stopping power the tracks are discontinuous (amorphous in some parts and crystalline in others). This is confirmed by the inset annular bright field scanning transmission electron micrograph, STEM (see Fig. 1b) of 220 MeV Xe tracks ($S_e \approx 22$ keV/nm) which shows those tracks in a planar orientation. The tracks encircled with solid lines are crystalline and those encircled with dashed lines are amorphous — for the part of the tracks which are in focus in this image. A rough estimate for tracks' size ($S_e \approx 22$ keV/nm) from Fig. 1b gives a value of between 1.5 and 2 nm.

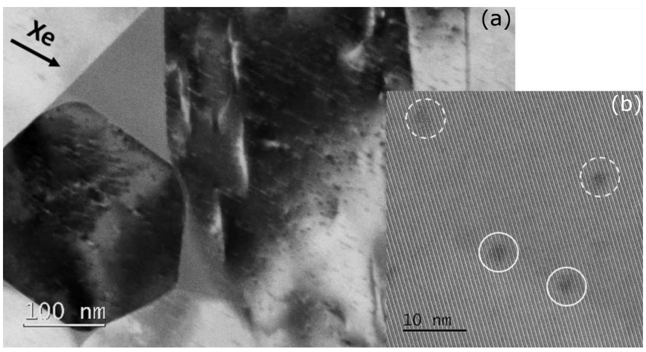

Fig. 1. (a) Bright field TEM micrograph of Al doped Si_3N_4 irradiated with 167 MeV Xe to a fluence value of 1×10^{12} cm^{-2}, (b) an annular bright field STEM micrograph of 220 MeV Xe to a fluence of 5×10^{11} cm^{-2} showing tracks in a planar orientation.

The threshold stopping power (S_{et}) is calculated from the plot of electronic stopping power (S_e) vs. depth simulated using the SRIM code [12] using the built-in values for pure Si_3N_4 and a density of 3.17 g cm^{-3} (Fig. 2). The depth to which 167 MeV Xe induced tracks remain visible in the TEM is measured and used as the value for the depth which determines S_{et}. This measurement yields a value for S_{et} of 8.9 keV/nm.

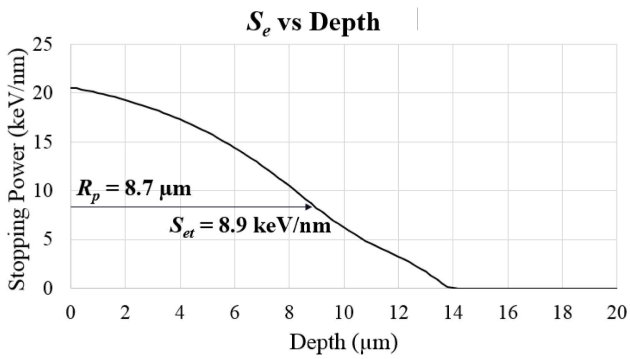

Fig. 2. TRIM calculation of electronic stopping power (S_e) of 167 MeV Xe in pure Si_3N_4.

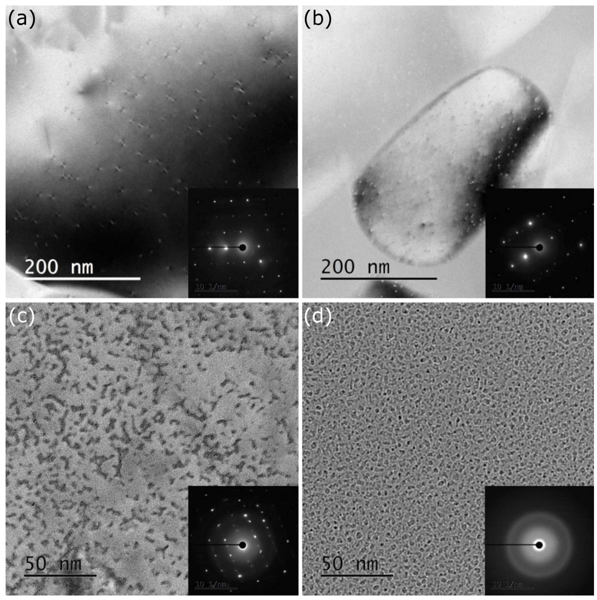

Fig. 3. Bright field TEM micrographs of Al doped Si_3N_4 irradiated with 220 MeV Xe to fluences of (a) 3×10^{11} cm^{-2}, (b) 5×10^{11} cm^{-2}, (c) 1×10^{13} cm^{-2}, (d) 2×10^{14} cm^{-2}. The insets in the bottom right corners are selected area diffraction patterns showing the evolution of the microstructure, with increasing ion fluence, toward full amorphisation.

At a fluence of 3×10^{11} cm^{-2} Al doped Si_3N_4 irradiated with 220 MeV Xe forms distinct latent tracks, as shown in Fig. 3a. The same is true at a slightly higher fluence of 5×10^{11} cm^{-2} (Fig. 3b) where only the number of latent tracks has increased. The inset diffraction patterns in the bottom right corners of Fig. 3a and b show that the material remains crystalline at these fluences and there is no contribution from small amount of amorphous material in the ion tracks as seen in Fig. 1. At a fluence of 1×10^{13} cm^{-2} (Fig. 3c) the material becomes highly strained and some tracks start to overlap. The inset diffraction pattern also contains a diffuse ring which indicates the presence of a significant amount of amorphous material — areas of dark contrast in the TEM micrograph. Finally, at a fluence of 2×10^{14} cm^{-2} (Fig. 3d) the material has become completely amorphous, as confirmed by the inset diffraction pattern.

To determine both the threshold fluence and stopping powers needed to induce amorphisation of Al doped Si_3N_4 cross-sectional TEM lamellae stretching from the surface to the maximum depth of implantation were produced for 220 MeV Xe to a fluence of 2×10^{14} cm^{-2} (Fig. 4) and for 167 MeV Xe to a fluence of 6×10^{14} cm^{-2} (Fig. 5). A clear amorphisation to crystalline boundary zone can be seen for 167 MeV Xe at 10.51 μm and for 220 MeV Xe at 12.75 μm, which corresponds to stopping powers of 6.8 and 8.1 keV/nm, respectively, calculated using SRIM for amorphous Si_3N_4.

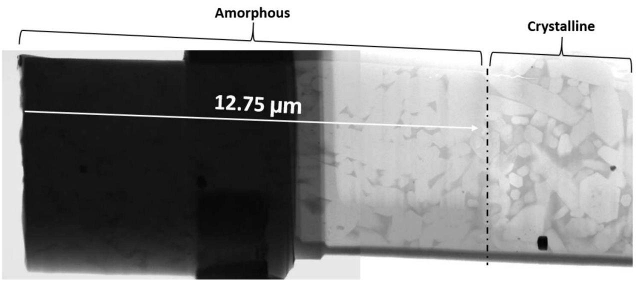

Fig. 4. A cross-sectional bright field TEM micrograph of Al doped Si_3N_4 irradiated with 220 MeV Xe to a fluence of 2×10^{14} cm^{-2}.

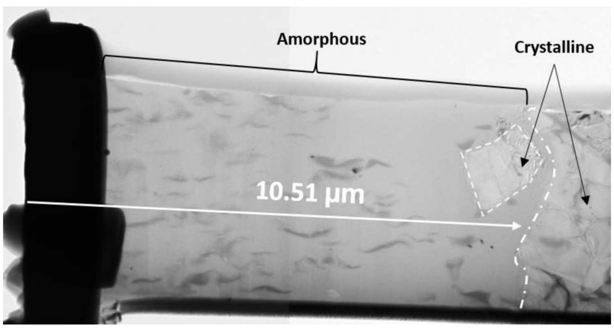

Fig. 5. A cross-sectional bright field TEM micrograph of Al doped Si_3N_4 irradiated with 167 MeV Xe to a fluence of 6×10^{14} cm^{-2}.

The current results show that total amorphisation through electronic stopping occurs at fluences greater than 1×10^{13} cm^{-2}. The sample irradiated with 167 MeV Xe contains a grain of mostly pure Si_3N_4, confirmed by EDS analysis, which lies within the depth that was amorphized (Fig. 6). This grain did not contain any latent ion tracks, only an indication of increased strain. The stopping power in this region where the grain is located lies between 6 and 8 keV/nm (calculated for am-Si_3N_4). The lack of tracks in this crystallite in part confirms the finding that S_{et} for pure Si_3N_4 is $>$ 15 keV/nm.

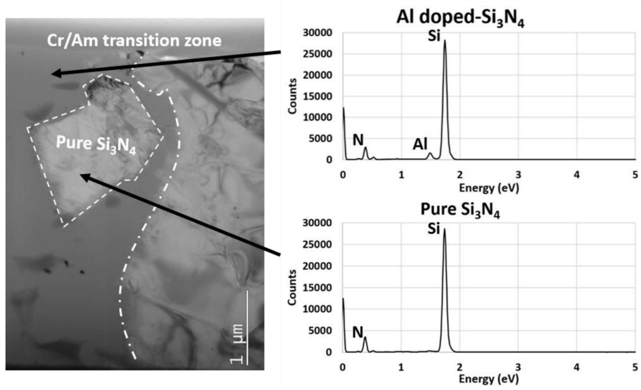

Fig. 6. A bright field TEM micrograph of the highlighted area (the amorphous/crystalline transition zone) in Fig. 5 showing a Si_3N_4 grain which does not contain Al and remains crystalline. TheEDS spectra were collected from both the pure-Si_3N_4 and Al doped-Si_3N_4 areas and clearly shows the absence of Al signal for the area designated as pure Si_3N_4.

4. Conclusions

The threshold stopping power for Al doped β-Si_3N_4 has been calculated from track depth measurements to be 8.9 keV/nm, which is lower than 15 keV/nm found by Zinkle et al. [13] for pure β -Si_3N_4 but much closer to the theoretically predicted value of 10.1 keV/nm by Szenes et al. [14].

The results of this investigation suggest that the onset of amorphisation in Al doped β -Si_3N_4 occurs at a fluence of 1×10^{13} cm^{-2} and complete amorphisation is observed at a fluence of 2×10^{14} cm^{-2}. At a fluence of 6×10^{14} cm^{-2} the sintering compound and grains even become deformed due to the high level of damage. The exact threshold fluence for amorphisation by electronic stopping however probably lies somewhere between 1×10^{13} and 2×10^{14} cm^{-2} (to be investigated). The results also suggest that a minimum stopping power of between 6.8 and 8.1 keV/nm is required to induce this amorphisation, since material beyond this critical value remains crystalline.

The promotion of amorphisation in Si_3N_4 due to doping with certain impurities has been observed by Zinkle et al. [15]. However, this was for Si_3N_4 irradiated with 2 MeV Si and amorphisation only occurred in the region where nuclear stopping was dominant. A convenient confirmation of this effect of doping on amorphisation threshold through electronic stopping is the clear crystalline grain of pure Si_3N_4 in a region of Al doped material which is completely amorphous.

References

[1] Y.W. Lee, C.Y. Joung, S.H. Kim, S.C. Lee, *Met. Mater. Int.* **7**, 159 (2001).

[2] C. Degueldre, J.M. Paratte, *J. Nucl. Mater.* **274**, 1 (1999).

[3] M. Toulemonde, C. Dufour, A. Meftah, E. Paumier, *Nucl. Instrum. Meth. Phys. Res. B* **166**, 903 (2000).

[4] S.L. Daraszewicz, D.M. Duffy, *Nucl. Instrum. Meth. Phys. Res. B* **269**, 1646 (2011).

[5] M. Kitayama, K. Hirao, M. Toriyama, S. Kanzaki, *J. Am. Ceram. Soc.* **82**, 3105 (1999) .

[6] F.L. Riley, *J. Am. Ceram. Soc.* **83**, 245 (2000).

[7] J. Yamane, M. Imai, T. Yano, *Prog. Nucl. Energy* **50**, 621 (2008).

[8] Z. Mao, Y. Zhu, Y. Zeng, F. Xu, Z. Liu, G. Ma, Z. Duc, W. Geng, *Cryst. Eng. Commun.* **14**, 7929 (2012).

[9] X.F. Lu, P. La, X. Guo, Y. Wei, X. Nan, L. He, *Comput. Mater. Sci.* **79**, 174 (2013).

[10] X.F. Lu, D. Qiu, M. Chen, L. Fan, C. Wang, H.J. Wang, G.J. Qiao, *Mater. Res. Innovat.* **17**, 201 (2013).

[11] S. Abroug, F. Saadallah, N. Yacoubi, *Eur. Phys. J. Spec. Topics* **153**, 29 (2008).

[12] J.F. Ziegler, M.D. Ziegler, J.P. Biersack, *Nucl. Instrum. Meth. Phys. Res. B* **268**, 1818 (2010).

[13] S.J. Zinkle, J.W. Jones, V.A. Skuratov, *Mater. Res. Soc. Symp. Proc.* **650**, R3.19 (2001).

[14] G. Szenes, *J. Nucl. Mater.* **336**, 81 (2005).

[15] S.J. Zinkle, L.L. Snead, W.S. Eatherly, J.W. Jones, D.K. Hensley, *Mater. Res. Soc. Symp. Proc.* **540**, 305 (1998).